REPORTS

Diffusion of Nonequilibrium Quasi-Particles in a Cuprate Superconductor

N. Gedik,[1] J. Orenstein,[1]* Ruixing Liang,[2] D. A. Bonn,[2] W. N. Hardy[2]

We report a transport study of nonequilibrium quasi-particles in a high-transition-temperature cuprate superconductor using the transient grating technique. Low-intensity laser excitation (at a photon energy of 1.5 electron volts) was used to introduce a spatially periodic density of quasi-particles into a high-quality untwinned single crystal of $YBa_2Cu_3O_{6.5}$. Probing the evolution of the initial density through space and time yielded the quasi-particle diffusion coefficient and the inelastic and elastic scattering rates. The technique reported here is potentially applicable to precision measurements of quasi-particle dynamics not only in cuprate superconductors but in other electronic systems as well.

Quasi-particles are the elementary excitations of a superconductor, created when a Cooper pair of electrons breaks apart. The dynamic properties of quasi-particles, that is, their rates of diffusion, scattering, trapping, and recombination, are critical for applications of conventional superconductors in x-ray detectors (*1*) and in the manipulation of superconductor-based qubits (*2*). In more exotic superconductors such as the high-transition-temperature (T_c) cuprates, a better understanding of quasi-particle dynamics may help to uncover the mechanism for Cooper pairing. A special property of the cuprate superconductors is the d-wave symmetry of the gap function, which leads to an unusual quasi-particle spectrum. The minimum energy for the creation of a quasi-particle depends on the direction of its momentum (*3*). It is zero for momenta in the "nodal" direction, oriented at 45° relative to the Cu-O bond. The most energetically expensive quasi-particles are the "antinodal" ones, whose momenta are nearly parallel to the bond. The antinodal quasi-particles are the mystery particles of cuprate superconductivity. Because they feel the pairing interaction most strongly, their properties may hold the key to high-T_c superconductivity. Unfortunately, their tendency to form strong pairs makes them difficult to study. In thermal equilibrium, the population of quasi-particles is overwhelmingly dominated by the low-energy nodal ones. As a result, transport measurements performed in equilibrium, such as microwave (*4*) and thermal (*5*) conductivity, are insensitive to antinodal quasi-particles.

In this work, a transient grating technique was developed and used to probe the transport of nonequilibrium quasi-particles in the high-T_c superconductor $YBa_2Cu_3O_{6.5}$. We find that the diffusion coefficient, D, is much smaller than the value obtained in measurements on equilibrium quasi-particles in the same material. The disparity in D suggests that the current experiment probes a population of quasi-particles that are not near the nodes and that are perhaps close to the antinodal regions of momentum space.

The nonequilibrium quasi-particles were introduced with the use of short optical pulses. To probe their propagation, we generated a spatially periodic population by interfering two pulses at the sample surface. The spatial period, λ_g, equals $\lambda/2\sin\theta$, where λ is the wavelength of the pulse and 2θ is the angle between the two pump beams. The nonequilibrium quasi-particles cause a change in the index of refraction at the laser frequency (*6*) that is a linear function of their density (*7*). As a result, the sinusoidal variation in quasi-particle density creates an index grating that can be detected by the diffraction of a probe pulse.

After creation, the distribution of quasi-particles evolves because of the combined effects of recombination and diffusion. In the process of recombination, a pair of quasi-particles jumps back into the Cooper pair condensate with the simultaneous transfer of their creation energy to some other form (e.g., phonons). The amplitude of the grating may also decay as quasi-particle diffusion drives the system toward a spatially homogeneous quasi-particle concentration. The goal of the experiment is to disentangle these effects and measure both the rates of recombination and diffusion.

The transient grating technique has been used successfully in a wide variety of applications, including exciton diffusion, dynamics of biomolecules, propagation of ultrasound, and thermal diffusion (*8*). Observing the propagation of superconducting quasi-particles requires the ability to detect the transient grating at extremely dilute concentrations. At the low excitation densities needed to detect their propagation, the quasi-particles produce a fractional change of no more than 10^{-5} in the index of refraction. The diffracted intensity from such a grating would therefore be on the order of 10^{-10} of the incident probe intensity and consequently very difficult to detect.

Detection of the grating required the measurement of the amplitude of the diffracted wave rather than the intensity. This is accomplished through the use of heterodyne detection (*9*, *10*). The key element in the success of the heterodyne technique is the diffractive optic (DO) beamsplitter, which creates pairs of pump and probe beams (*11*, *12*). The DO element in our experimental setup (Fig. 1) is an array of 10 separate square phase masks (2.5 mm on a side), each with a different grating period, on a fused silica substrate. A beam from a Ti:sapphire laser (λ = 800 nm and pulse repetition rate of 80 MHz) is split into primary pump and probe beams, which are focused onto one of the phase masks at a small angle with respect to each other. The phase mask splits each of the primary beams by diffraction into the $m = \pm 1$ orders. (For clarity, only the probe beam paths are shown in Fig. 1.)

The interference of the two pump beams creates a spatially varying index of refraction in the sample that reaches a depth of 1000 Å below the surface and has half the period of the phase mask. We detect the index variation with the use of an implementation of the heterodyne technique that enables absolute calibration of the phase (*13*). Each of the two probe beams is specularly reflected from the surface of the sample and returns via the DO to a Si detector. The two possible round-trip beam paths are shown as solid and dashed lines in Fig. 1. With the use of the DO beamsplitter, detection of the diffracted probe is automatically aligned. The diffracted component of P1 is precisely colinear with reflected P2 and vice versa. The experiment is performed by alternately blocking one of the two reflected beams. If reflected P1 is blocked, then reflected P2 and diffracted P1 are mixed in the detector. This measurement by itself is insufficient to extract the wave amplitudes, because the phase difference between P1 and P2 is undetermined. However, simply blocking reflected P2 instead of P1 produces a mixed signal with the conjugate phase. Comparing the detector output

[1]Physics Department, University of California, Berkeley, and Materials Science Division, Lawrence Berkeley National Laboratory, Berkeley, CA 94720, USA. [2]Department of Physics and Astronomy, University of British Columbia, Vancouver, British Columbia V6T 1Z1, Canada.

*To whom correspondence should be addressed. E-mail: joeo@mh1.lbl.gov

for the two conjugate beam paths fixes the absolute phase and therefore the wave amplitudes as well.

By adjusting the phase delay of P1 relative to P2, the output of the Si photodiode measures either the change of the specular reflection coefficient due to the grating, R, or the amplitude of the diffraction efficiency, TG. R is proportional to the spatial average of the quasi-particle concentration, whereas TG is proportional to the component of the quasi-particle concentration at the fundamental period of the grating, λ_g (*14*). In Fig. 2, we plot both R and TG for λ_g = 2 μm as a function of time delay for several intensities of the excitation pulses and consequently for a range of initial quasi-particle concentrations. The temperature of the sample was 5 K, and the grating wave vector was oriented along the crystallographic **b** axis (parallel to the Cu-O chains).

The curves are normalized to their value at time delay zero. The R curves, which decay because of recombination, are nonexponential, and their characteristic rate of decay increases with increasing concentration (*7*). The increase of recombination rate with density is consistent with the idea that each quasi-particle must encounter another to scatter into the Cooper pair condensate. The corresponding TG curves depend strongly on the pump intensity as well. However, the time dependence at each pump intensity is different from R, because TG reflects the combined effects of recombination and propagation. In systems where the recombination rate is independent of density, it is relatively straightforward to separate the effects of particle decay and diffusion. If the average concentration decays exponentially with rate γ, the amplitude of the grating decays with rate $\gamma + Dq^2$, where D is the diffusion coefficient and q is the wave vector of the grating, $2\pi/\lambda_g$. The ratio TG/R, which decays simply as $\exp(-Dq^2t)$, isolates the effects of diffusion on the evolution of the particle density.

With this example in mind, we are led to consider TG/R for our data (Fig. 3). Figure 3, A and B, show TG/R for grating periods of 2 and 5 μm, respectively, for several values of the pump laser intensity. Unlike the example of density-independent recombination, the decay of TG/R is nonexponential and highly dependent on the excitation density. At high intensity, TG/R recovers its value at zero time delay after an initial rapid decrease. TG/R is nearly independent of grating period at high intensity. As intensity decreases, the minimum of TG/R moves systematically toward longer times, and the decay approaches a simple exponential. The exponential rate at low pump laser intensity depends strongly on λ_g, as is expected if the grating decays because of diffusion.

The dependence of TG/R on laser intensity and grating period results from an interplay of density-dependent recombination, diffusion, and energy transfer. To unravel these effects, we have modeled the quasi-particle dynamics by adding a quadratic recombination term to the diffusion equation $\partial n(x, t)/\partial t = D\partial^2 n(x, t)/\partial x^2 - \beta n^2(x, t)$ (*13*). Here, n is the quasi-particle density and β is the recombination coefficient, which is a measure of the inelastic scattering rate (*15*). The dynamics predicted by this equation depend on the relative magnitude of βn and Dq^2. In the high-density regime $\beta n \gg Dq^2$, recombination dominates over diffusion. Because the rate is more rapid where n is larger, recombination distorts the sinusoidal grating by flattening the crests. The distortion of the grating profile reduces the component of n at the fundamental grating period faster than its spatial average. This accounts for the initial decrease of TG/R. However, if this were the only process, TG/R would never bounce back to its initial value, as it is seen to do in Fig. 3.

TG/R recovers in the high-intensity regime because the energy released as the quasi-particles recombine appears in another form, one that also creates a change in the index of refraction. In conventional superconductors, the quasi-particle energy is converted to lattice vibrational energy, which (in the presence of electron-phonon coupling) will change the index. Although phonons may play this role in the cuprate superconductors as well, excitations involving the flipping of electron spins may be generated instead when quasi-particles recombine (*16*). In either case, the recovery of TG/R follows if this secondary form of energy does not diffuse on the 100-ps time scale. In this case, the original sinusoidal distribution of energy is written into a stationary form of energy before the quasi-particles have had a chance to diffuse. When almost all the energy has been handed off from the quasi-particles to nonpropagating modes, the grating recovers its sinusoidal

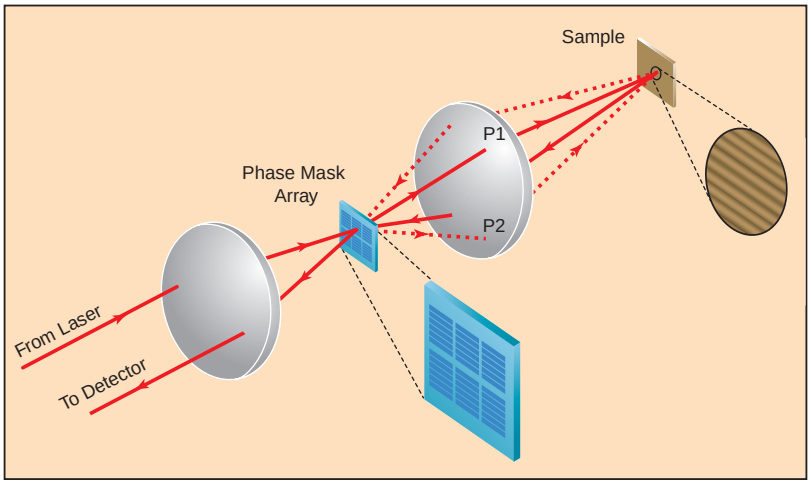

Fig. 1. Illustration of the beam path for heterodyne transient grating detection. Pump and probe beams from the laser are split at the diffractive optic (for clarity, only the probe beams are shown). A spherical mirror and a plane folding mirror (represented schematically by the second lens in the sketch) focus the beams to a single 100-μm spot on the sample. After specular reflection and diffraction at the sample surface, the two probe beams are recombined by the diffractive optic and directed to a Si photodiode detector. The wave vector of the quasi-particle density variation is changed without optical realignment by translating the diffractive optic so that a different phase mask in the array is inserted in the beam.

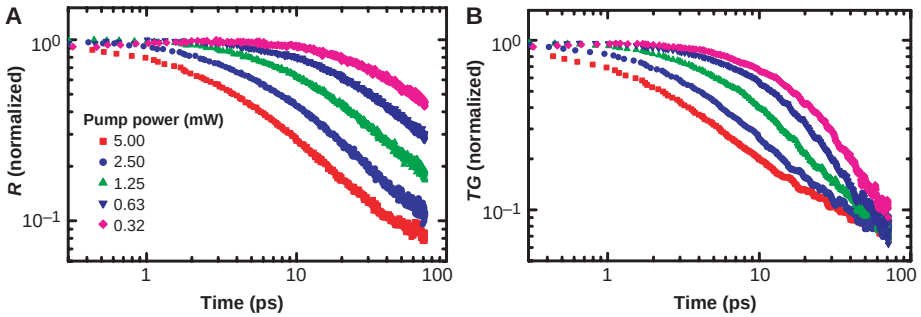

Fig. 2. (**A**) Change in the specular reflection coefficient, R, as a function of the time delay after creation of the grating for several values of the pump intensity. R is normalized to unity at time delay zero to illustrate the systematic slowing down of the recombination rate as the excitation density is decreased. (**B**) Normalized amplitude of the diffracted probe beam as a function of time delay for the same values of pump intensity used to measure R.

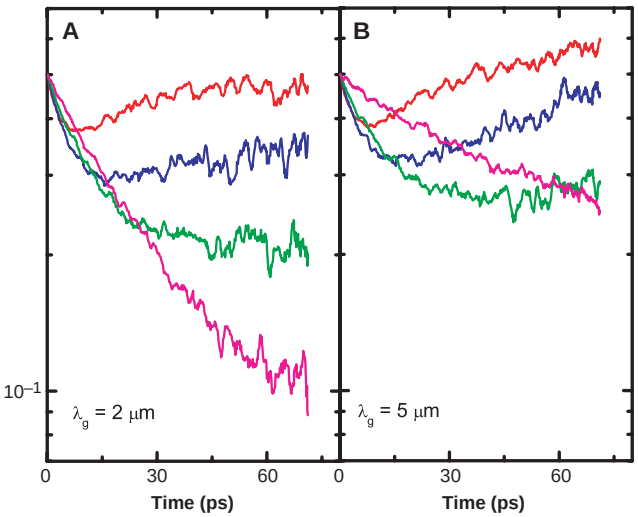

Fig. 3. The ratio *TG/R* for the same pump intensities as in Fig. 2 (with $P = 0.63$ mW omitted for clarity) for the grating periods of 2 μm (**A**) and 5 μm (**B**). At high excitation density, the curves are nearly independent of the period. At low excitation density, the grating enters the propagation-dominated regime where the decay of *TG/R* depends strongly on the period of the grating.

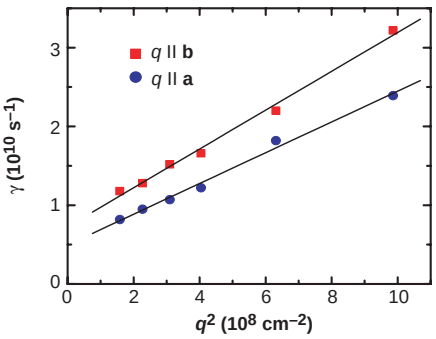

Fig. 4. Initial decay rate of *TG/R* for the same low intensity as in Fig. 3, plotted as a function of the square of the grating wave vector. Results are shown for two perpendicular orientations of the grating. The linear dependence of the rate on q^2 demonstrates that the propagation is diffusive. The slopes of linear fits yield diffusion coefficients $D_a = 20$ cm^2/s and $D_b = 24$ cm^2/s.

profile and *TG/R* returns to its value at time zero. The energy remains frozen until the nanosecond time scale, when thermal diffusion finally leads to decay of the grating (*17*).

The effects of diffusion dominate in the low-density regime, $\beta n \ll Dq^2$, where quasi-particle motion washes out the grating before energy transfer can take place. According to the equation governing $n(x, t)$, *TG/R* becomes q dependent and intensity independent in this limit. To find the rate of diffusion, we measured *TG/R* at low power ($P = 0.32$ mW) for several grating periods between 2 and 5 μm. The initial decay rate of *TG/R* at low power is plotted as a function of q^2 in Fig. 4. The decay rate depends systematically on the grating period, demonstrating that the dynamics are in the propagation-dominated regime. The rates for the grating oriented along both the **a** and **b** crystallographic directions are plotted. For both directions, the rate is a linear function of q^2, demonstrating that the quasi-particle propagation is diffusive. From the slope of a linear fit, we determine that $D_a = 20$ cm^2/s and $D_b = 24$ cm^2/s. The intercept as q tends to zero is the decay rate due to recombination.

It is possible to infer the mean free time, τ, and mean square velocity, $\langle v^2 \rangle$, of nonequilibrium quasi-particles from the values of D quoted above. A lower bound on τ is obtained by inserting the maximum quasi-particle velocity, the Fermi velocity, v_F, into the kinetic formula $D = \langle v^2 \rangle \tau/2$. The literature value (*18*) of v_F, 2×10^7 cm/s, yields a lower bound of 100 fs. An upper bound on τ of essentially the same value can also be inferred from the experiment. If τ were much longer than 100 fs, then quasi-particle propagation would be ballistic on the subpicosecond time scale. However, the time and wave vector dependence of *TG* proves that quasi-particle motion is diffusive at the earliest times we can resolve, which is ~ 300 fs after creation of the grating. Thus, the allowed values of τ and v are narrowly bracketed near 100 fs and v_F, respectively. Furthermore, the measurements indicate that τ is determined by elastic rather than inelastic processes. The nonequilibrium particles survive for ≈100 ps and therefore scatter ≈1000 times before decaying. This would be impossible if each scattering event resulted in a substantial reduction of the quasi-particle's energy.

Equilibrium measurements find (in the same crystal and at the same temperature) that τ = 20 ps (*19*), which is 200 times longer than τ values of the nonequilibrium quasi-particles. The contrast suggests that the nonequilibrium quasi-particles are different from those present in thermal equilibrium. The equilibrium particles occupy states that have a small energy (k_BT) relative to the chemical potential and therefore lie very near the gap nodes. If the nonequilibrium quasi-particles are different, they must occupy higher energy states, perhaps ones closer to the antinodal regions of momentum space. It is possible that the constraints of momentum and energy conservation prevent relaxation of antinodal quasi-particles to the nodal regions. If the particles are antinodal, it is relevant to compare the width of the antinodal quasi-particle peak as measured by photoemission with $\hbar/\tau$ as measured by nonequilibrium transport. The peak width of 14 meV (*20*) corresponds to τ = 50 fs, which is close to the transport value, particularly considering that photoemission is performed on $Bi_2Sr_2CaCu_2O_8$ rather than $YBa_2Cu_3O_{6.5}$. The similarity of lifetimes suggests that the peak width in photoemission may be controlled by elastic scattering as well.

The transient grating method reported here promises to be broadly applicable to superconductors as well as other materials in which there is a gap in the quasi-particle spectrum. The technique works readily in transmission or reflection geometry and therefore can be applied to bulk materials or thin films. The propagation of quasi-particles can be tracked in any system where nonequilibrium excitations generate a change in the index of refraction at the laser wavelength. In conventional superconductors, quasi-particle diffusion can be measured without fabricating trapping layers and junction detectors. In more exotic systems with multiple or anisotropic gaps such as reported in this paper, the transient grating technique can track the propagation of quasi-particles that conventional transport methods cannot detect.

References and Notes

1. N. E. Booth, D. J. Goldie, *Supercond. Sci. Technol.* **9**, 493 (1996).
2. K. M. Lang, S. Nam, J. Aumentado, C. Urbina, J. M. Martinis (2002), preprint available at www.boulder.nist.gov/div814/div814/pubs/downloads/qcompute/jmm-ASCO2preprint.pdf.
3. Z. X. Shen *et al.*, *Phys. Rev. Lett.* **70**, 1553 (1993).
4. A. Hosseini *et al.*, *Phys. Rev. B* **60**, 1349 (1999).
5. Y. Zhang *et al.*, *Phys. Rev. Lett.* **86**, 890 (2001).
6. J. M. Chwalek, C. Uher, J. F. Whitaker, G. A. Mourou, J. A. Agostinelli, *Appl. Phys. Lett.* **58**, 980 (1990).
7. G. P. Segre *et al.*, *Phys. Rev. Lett.* **88**, 137001 (2002).
8. H. J. Eichler, P. Gunter, D. W. Pohl, *Laser-Induced Dynamic Gratings* (Springer-Verlag, Berlin, 1986).
9. P. Vohringer, N. F. Scherer, *J. Phys. Chem.* **99**, 2684 (1995).
10. Y. J. Chang. P. Cong. J. D. Simon, *J. Phys. Chem.* **99**, 7857 (1995).
11. G. D. Goodno, G. Dadusc, R. J. D. Miller, *J. Opt. Soc. Am. B* **15**, 1791 (1998).
12. A. A. Maznev, K. A. Nelson, T. A. Rogers, *Opt. Lett.* **23**, 1319 (1998).
13. Details of experimental methods and theoretical modeling are available as supporting material on *Science* Online.
14. I. M. Fishman, C. D. Marshall, M. D. Fayer, *J. Opt. Soc. Am. B* **8**, 1880 (1991).
15. S. B. Kaplan *et al.*, *Phys. Rev. B* **14**, 4854 (1976).
16. S. M. Quinlan, D. J. Scalapino, N. Bulut, *Phys. Rev. B* **49**, 1470 (1994).
17. C. D. Marshall, I. M. Fishman, R. C. Dorfman, C. B. Eom, M. D. Fayer, *Phys. Rev. B* **45**, 10009 (1992).
18. T. Valla *et al.*, *Phys. Rev. Lett.* **85**, 828 (2000).
19. P. J. Turner *et al.*, preprint available online at http://xxx.lanl.gov/abs/cond-mat/0111353.
20. A. V. Fedorov *et al.*, *Phys. Rev. Lett.* **82**, 2179 (1999).

21. This work was supported by DOE-DE-AC03-76SF00098, Canadian Institute for Advanced Research, and Natural Sciences and Engineering Research Council of Canada.

Supporting Online Material

www.sciencemag.org/cgi/content/full/300/5624/1410/DC1

Materials and Methods

Figs. S1 to S3

3 February 2003; accepted 15 April 2003